SEISMIC HAZARD OF THE CANTERBURY REGION, NEW ZEALAND: NEW EARTHQUAKE SOURCE MODEL AND METHODOLOGY

Mark Stirling[1], Matthew Gerstenberger[1], Nicola Litchfield[1], Graeme McVerry[1], Warwick Smith[1], Jarg Pettinga[2] and Philip Barnes[3]

SUMMARY

We present a new probabilistic seismic hazard model for the Canterbury region, the model superseding the earlier model of Stirling *et al.* (1999, 2001). The updated model incorporates new onshore and offshore fault data, new seismicity data, new methods for the earthquake source parameterisation of both datasets, and new methods for estimation of the expected levels of Modified Mercalli Intensity (MMI) across the region. While the overall regional pattern of estimated hazard has not changed since the earlier seismic hazard model, there have been slight reductions in hazard in some areas (western Canterbury Plains and eastern Southern Alps), coupled with significant increases in hazard in one area (immediately northeast of Kaikoura). The changes to estimated acceleration for the new versus older model serve to show the extent that major changes to a multidisciplinary source model may impact the final estimates of hazard, while the new MMI estimates show the added impact of a new methodology for calculating MMI hazard.

INTRODUCTION

We present the results of a new probabilistic seismic hazard assessment (PSHA) for the Canterbury region. The study represents an update of the comprehensive PSHA carried out for Environment Canterbury (ECan) in 1999 (Stirling *et al.* 1999, 2001), and also will contribute to an update of the national seismic hazard model (Stirling *et al.* 2002, 2007). The PSHA is carried out in much the same way as the older analysis, in that we combine geologic data describing the geometry and activity of the known active earthquake source faults in and around the Canterbury region with historical seismicity data to develop maps and site-specific estimates of expected earthquake shaking across the region.

The update of the PSH model comprises new onshore and offshore fault data (the latter were only minimally considered in the older study), the use of improved methods to estimate the recurrence parameters for active faults, and the use of a new distributed seismicity model that incorporates the historical catalogue data accumulated since the older model was developed. Our PSH maps show the peak ground accelerations (PGAs) and 5% damped response spectral accelerations (1 second periods) for 475 and 1,000 years for uniform Class C shallow soil site conditions (Standards New Zealand, 2004) calculated using the McVerry *et al.* (2006) attenuation model. MMIs are provided for the same return periods. We also show site-specific PSHAs for several towns or cities (Kaikoura, Christchurch and Timaru). Differences between the updated hazard estimates and those of the 1999 study are due to the combined effects of the new input data and methods. In subsequent text we refer to the Stirling *et al.* (1999, 2001) Canterbury PSH model as the "1999 study" or "1999 model", and the Stirling *et al.* (2002) New Zealand PSH model as the Stirling *et al.* (2002) model or study, or simply the national seismic hazard model. In this paper we only show selected maps, site-specific hazard calculations and de-aggregation plots, rather than the much fuller range of materials presented in the Stirling *et al.* (2007) report.

ACTIVE TECTONICS AND HISTORICAL SEISMICITY

As summarised in Stirling *et al* (2001, 2007), much of the Canterbury region is located within a wide zone of active earth deformation associated with oblique collision between the Australian and Pacific plates, where relative plate motion is obliquely convergent across the plate boundary at about 40 mm/yr at the latitude of Canterbury (De Mets *et al.* 1990; Fig. 1). The oblique collision is largely accommodated by the Alpine Fault to the west of the Canterbury region (Faults 7 and 8 in Fig. 2), where dextral slip rates of 15-35 mm/yr and uplift rates of the order 10 mm/yr are observed (e.g. Berryman &,

[1]*GNS Science, PO Box 30-368, Lower Hutt*

[2]*Natural Hazards Research Centre, Department of Geological Sciences, University of Canterbury, Private Bag, 4800, Christchurch*

[3]*National Institute of Water and Atmospheric Research, Greta Point Private Bag, Wellington*

Beanland 1988; Berryman *et al.* 1992; Sutherland & Norris, 1995; Norris & Cooper, 2001), and by dextral slip rates ranging from about 5 to 27 mm/yr on the Marlborough faults in the north of the region (the Wairau, Awatere, Clarence and Hope Faults; Langridge *et al.* 2003; faults 1-4, 9-14, and 20-21 in Fig. 2). The remaining component of plate motion is distributed widely across the central and southern parts of the region, and is expressed by the presence of strike-slip and reverse faults with slip rates of the order 1 mm/yr or less (Pettinga *et al.* 1998, 2001).

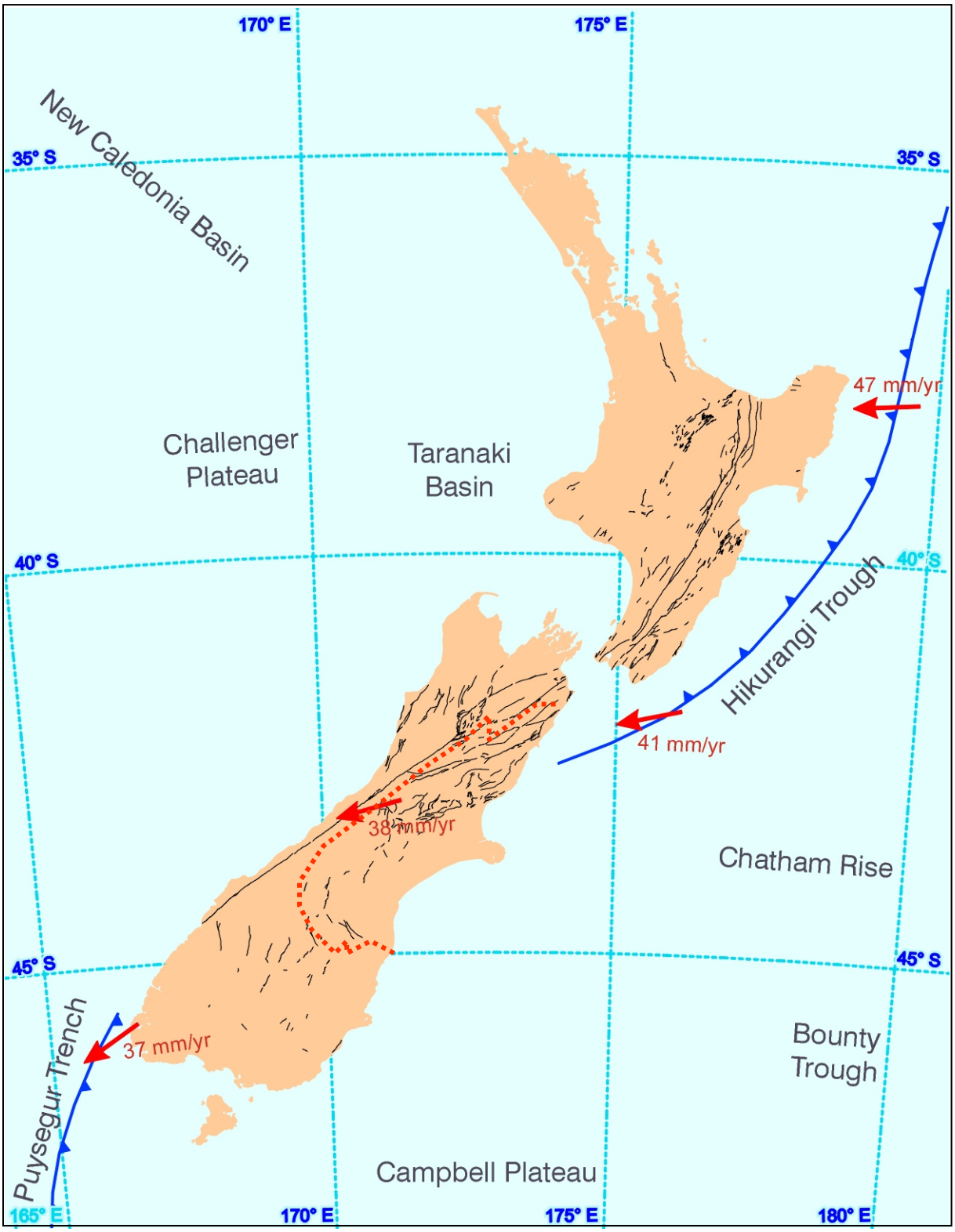

Figure 1. ***The plate tectonic setting of New Zealand, showing the relative plate motions (arrows with rates shown in mm/yr), major active fault traces, and the approximate boundary of the Canterbury region (dotted line).***

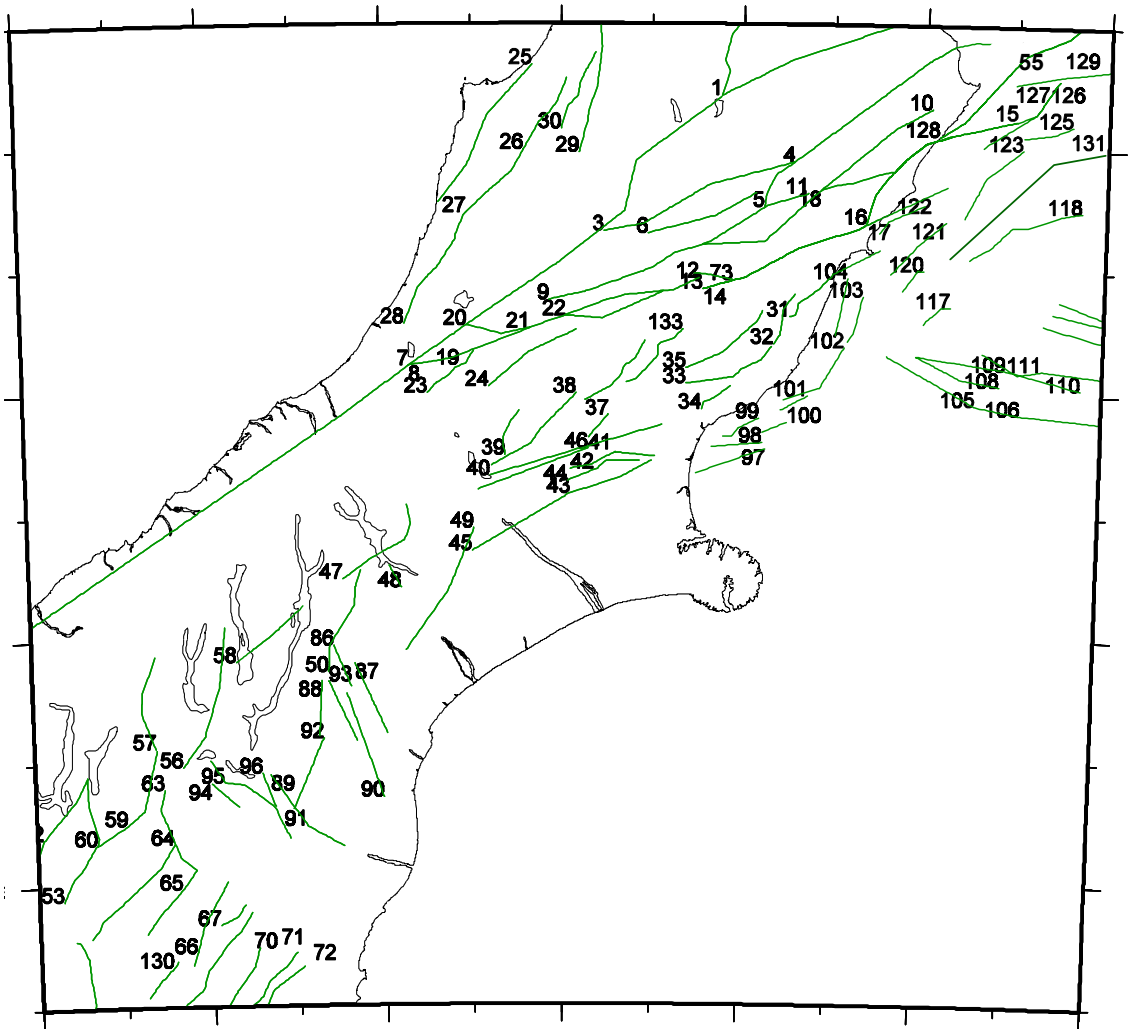

Figure 2a. ***The active fault sources used in the new model. The index numbers correspond to the last column in the Appendix, and are positioned at one end of each of the sources.***

Historical seismicity (Fig. 3) is most prolific in the northern and western parts of the Canterbury region, where there is also geological evidence of widespread active earth deformation. Several moderate-to-large ($M \geq 6.5$) shallow (≤ 15 km) earthquakes have occurred in the Canterbury and Marlborough regions since the inception of historical records in 1840. The earliest of these earthquakes was the M7.5 1848 Marlborough earthquake, which ruptured the northeastern section of the Awatere Fault (Grapes *et al.* 1998). The M7 - 7.3 1888 North Canterbury earthquake ruptured the central section of the Hope Fault (e.g. Cowan, 1991; Pettinga *et al.* 1998, 2001). Also, the Poulter Fault (Fault 24 in Fig. 2) has been defined as the source of the M7.0 - 7.1 1929 Arthur's Pass earthquake (Berryman & Villamor 2004). Aside from these earthquakes, no other ground rupturing earthquakes have occurred in the region in historic time. Geological investigations along the Alpine Fault provide evidence for the occurrence of great earthquakes ($M \geq 8$) with recurrence intervals of a few hundred years (e.g. Yetton *et al.*, 1998; Sutherland *et al.* 2006a & b), so the present lack of activity along the fault is due to the historic period coinciding with the time between these earthquakes.

Seismotectonic zonation of the Canterbury region is based on the zones defined for the national seismic hazard model (Stirling *et al.* 2002). This differs from the 1999 study, which divided the region into six structural domains according to Pettinga *et al.* (1998). The zones we use are shown in Figure 4. Use of the Stirling et al (2002) zones is for consistency of approach to that of the national seismic hazard model.

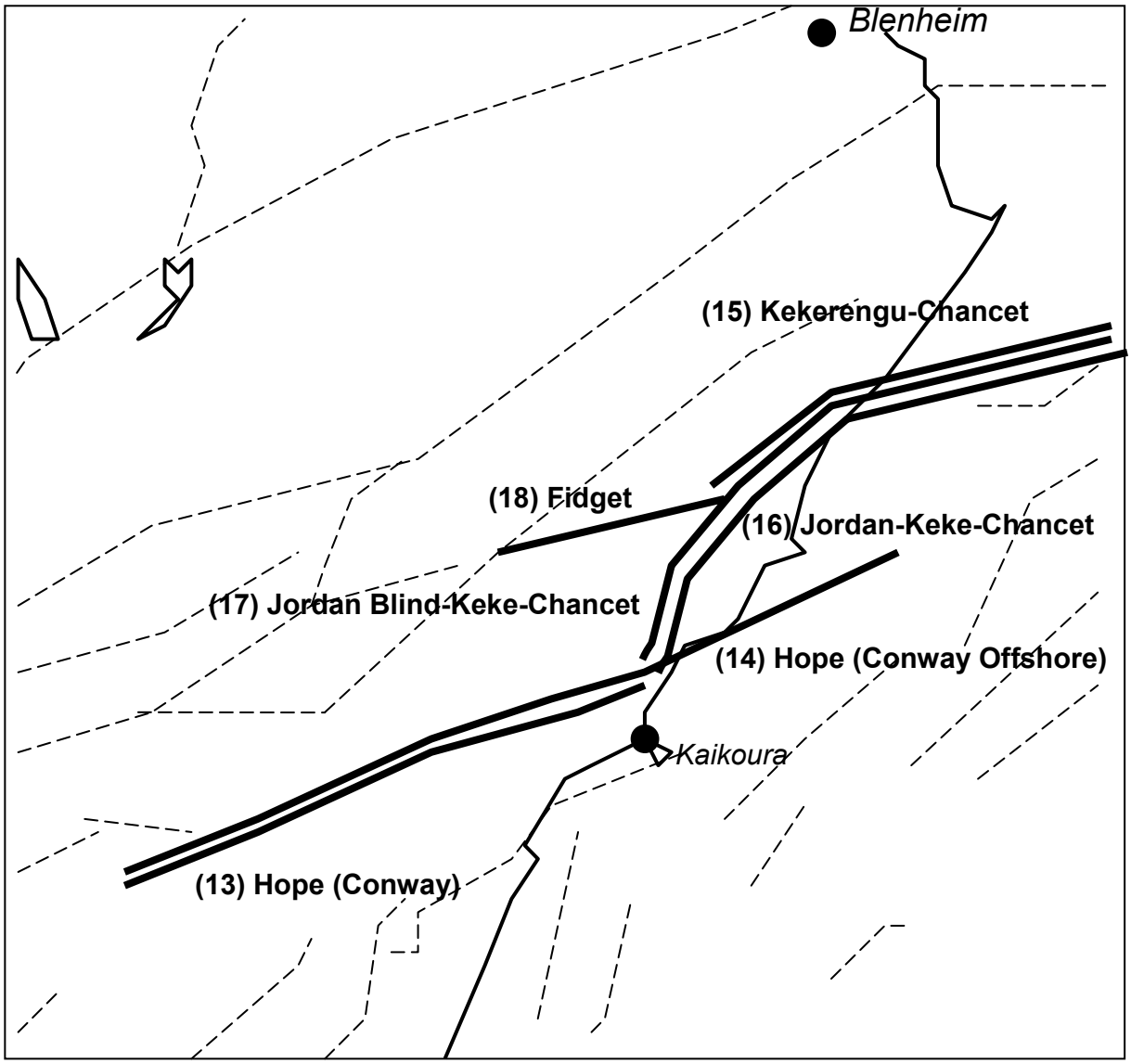

Figure 2b. ***The new active fault sources of northeastern Canterbury developed in the new model by Russ Van Dissen of GNS Science. Overlapping sources are shown side-by-side to distinguish them from one-another, and the index numbers correspond to the last column in the appendix.***

PROBABILISTIC SEISMIC HAZARD ANALYSIS

Method and Analysis

The PSHA methodology of Cornell (1968) forms the basis for our analysis. The steps taken to undertake our PSHA are: (1) use geologic data and the historical earthquake record to define the locations of earthquake sources and the likely magnitudes and frequencies of earthquakes that may be produced by each source; and (2) estimate the ground motions that the sources will produce at a grid of sites that covers the entire region. The computation of ground motions in (2) is achieved with a seismic hazard computer code corresponding to that developed by Stirling *et al.* (2002).

Earthquake Sources

Faults

We show the fault sources used in our PSHA in Figure 2, and list them in the Appendix. The new fault data (used to develop the fault source parameters in Stirling *et al.*, 2007) are obtained from the GNS active fault database (http://data/gns.cri.nz/af/), from recent field notes and recently completed university theses at the University of Canterbury, and from the National Institute of Water and Atmospheric Research (NIWA) offshore active fault database. Fault sources surrounding the Canterbury region have also been included as input to the PSHA, since these have the potential to contribute to the hazard inside the boundaries of the region. Much of the

update of the fault model has happened by way of a series of meetings of an expert panel based at GNS Science, NIWA and the University of Canterbury over the period July 2006 to January 2007 for onshore faults, and 2002 to 2007 for offshore faults (see Acknowledgements for a complete list of contributors). Considerable attention has also been given to reconciling plate motion rates with cumulative slip rates across the region, and onshore-offshore correlations of faults and slip rates. The fault traces shown on Figure 2 are generalisations of the mapped fault traces. These generalised representations are appropriate for regional scale PSHA. Unlike the 1999 study, we use a single method for estimating the likely characteristic magnitude (M_{max}) and recurrence interval of M_{max} earthquakes for each fault source in Figure 2.

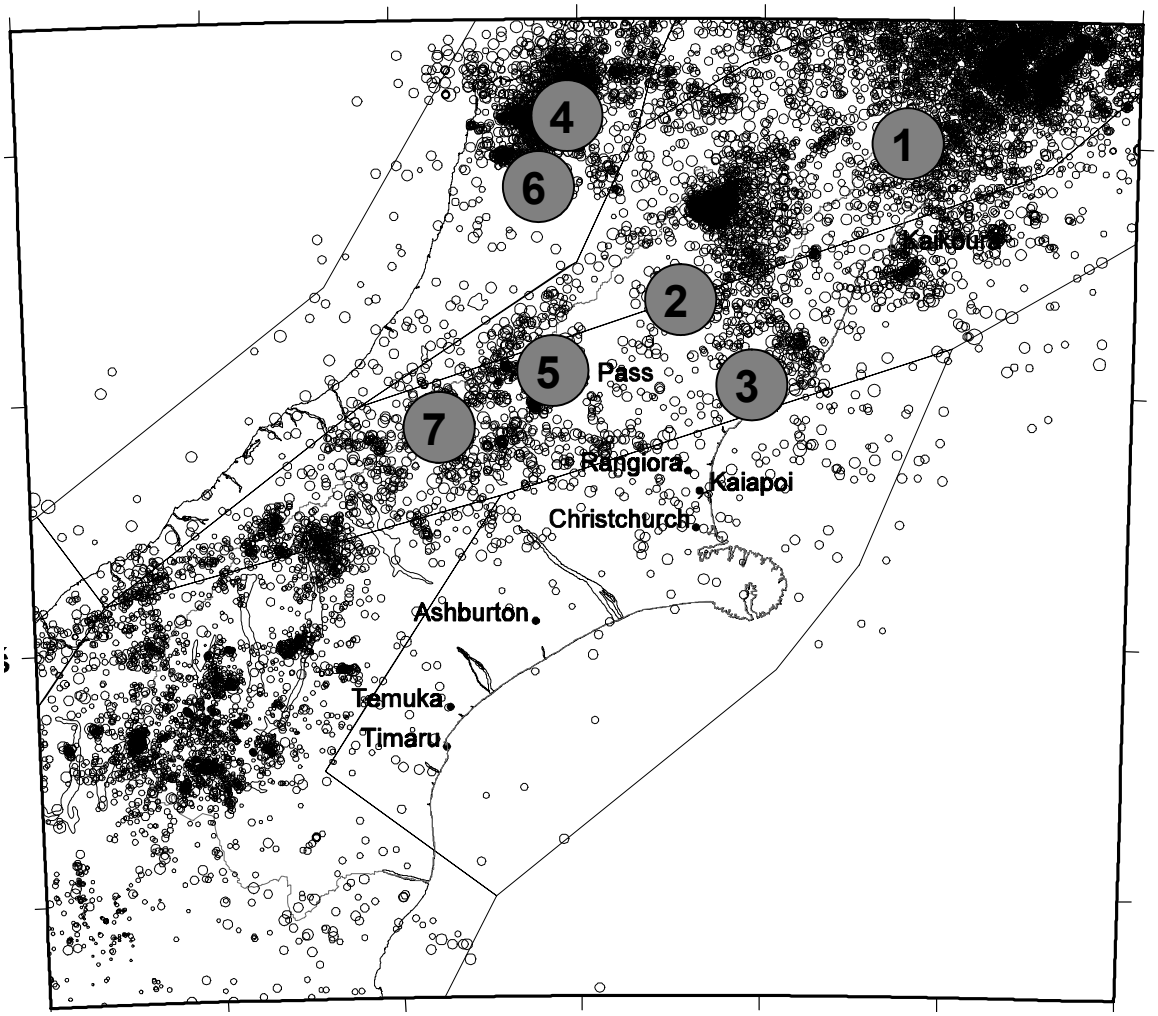

Figure 3. Historical seismicity of the Canterbury region. The map shows all earthquakes that have been historically observed and/or instrumentally recorded from 1900 to 2006 (source: www.geonet.org.nz). Shallow crustal historical earthquakes of M ≥ 6.5 are shown for the time-span 1840 to the present, and are as follows (numbered according to those shown on the map):

1. M7.5 1848 Marlborough
2. M7.1 1888 North Canterbury
3. M6.9 1901 Cheviot
4. M7.8 1929 Buller
5. M7.1 1929 Arthur's Pass
6. M6.7 1968 Inangahua
7. M6.7 1994 Avoca

This method utilizes newly developed regression equations of moment magnitude (M_w) on fault area for New Zealand earthquakes (Villamor *et al.* 2001; Berryman *et al.* 2002), an internationally-based regression for plate boundary strike-slip faults (Hanks & Bakun 2002), and a method for calculating recurrence interval that was developed by the expert panel for update of the national seismic hazard model. The method was largely developed by Villamor *et al.* (2001) and Berryman *et al.* (2002). The equations and method are as follows:

$$M_w = 4.18 + 2/3\log W + 4/3\log L \quad (1)$$

for New Zealand reverse and oblique-slip earthquakes (Berryman *et al.* 2002), in which W is fault width in km, and L is fault length in km

$$M_w = 3.39 + 1.33\log A \quad (2)$$

for New Zealand normal-slip earthquakes (Villamor *et al.* 2001), in which A is the fault area in km^2

$$M_w = 3.09 + 4/3\log A \quad (3)$$

for global plate boundary strike-slip earthquakes (Hanks & Bakun, 2002), in which A is the fault area in km^2

$$\log M_o = 16.05 + 1.5\, M_w \quad (4)$$

for global earthquakes (Hanks & Kanamori, 1979), in which M_o is seismic moment and M_w is moment magnitude

$$M_o = uLWD \quad (5)$$

for global earthquakes (Aki & Richards, 1980), in which uLWD are rigidity modulus (3×10^{11} dyne/cm^2), fault length (cm), fault width (cm) and single event displacement (cm), respectively.

$$RI = D/SR \quad (6)$$

for all earthquakes, in which RI is recurrence interval (years), D is single event displacement (mm) and SR is slip rate (mm/yr)

The procedure for parameterisation of the fault sources is to estimate magnitude (M_w) from fault dimensions according to the most appropriate choice of Equations 1 to 3, use Equation 4 to estimate the seismic moment (M_o) of the earthquake, Equation 5 to solve for the single event displacement (D) of the earthquake, and Equation 6 to solve for the recurrence interval (RI) from D and the slip rate (SR). The derived recurrence interval is then checked (validated) against the paleoseismic data for that fault, and discrepancies are then reduced or eliminated by adjustment of the parameters. The new procedure provides a single general method for the parameterisation of fault sources, and is iterative, in that it involves the validation and subsequent adjustment of the derived recurrence intervals (RI) according to paleoseismic data until consensus agreement on the suitability of the parameters is reached. In the new parameterisation, many of the old sources in the 1999 report are combined and/or lengthened for equations 1 to 6 to produce recurrence intervals consistent with paleoseismic data. The reduction or lengthening of sources is done carefully and in a manner consistent with regional neotectonics and structure. Sources are also drawn to closely match the actual fault traces. The new parameterisation has the benefit of eliminating the undesirable discrepancies and relatively short recurrence intervals that arose from the earlier methodology, which used different approaches to source parameterisation according to the quantity and quality of available data (an adaptation of the methodology used by the Working Group of California Earthquake Probabilities, 1995). Fewer fault sources exist in the new model as a result of the new methodology being applied to onshore Canterbury. Virtually all of the offshore faults used in the model (derived from NIWA) are new since the 1999 model was developed, and all have been parameterised according to the methodology outlined by equations 1 to 6 (above). The few offshore sources in the 1999 report have been substantially modified as a result of the new NIWA input. While validation of the resulting source parameters against paleoseismic data was not possible for the offshore faults, the offshore lengths, magnitudes and recurrence intervals were able to be assessed based on knowledge gained for the onshore faults. The faults are listed in the Appendix and shown in Figure 2.

It is worthwhile to briefly describe the most notable changes to the fault source model from the 1999 report. The source modelling for the Porters Pass Fault zone (referred to as "Porters to Grey" and fault 40 in the Appendix and Fig. 2a) has been simplified from the 1999 report. A single through-going Porters Pass Fault zone source is defined for our PSHA, replacing the equally-weighted through-going and segmented Porters Pass models that were used together in the 1999 model (Pettinga *et al.* 1998, 2001). The generally short sources defined for the segmented model in the 1999 report were the Mt Grey, Mt Thomas, and Porters Pass-Coopers Ck-Glentui-Townshend sources (Stirling *et al.*, 1999; 2001), all of which are amalgamated in our new model. Our methodology produces recurrence intervals that best match the paleoseismically-derived estimates of recurrence interval when a single through-going Porters Pass source is defined (Howard, 2001; Howard *et al.* 2005), as opposed to the very short recurrence intervals produced by the segmented model in the 1999 report. In terms of magnitude, a single $M > 7$ earthquake size is defined for the Porters Pass source, therefore eliminating the M6.5 - 7 earthquakes defined in the 1999 report.

The faults beneath the Canterbury Plains have been redefined and parameterised based on new data from the University of Canterbury. The relevant faults are the Ashley, Springbank, Cust, Hororata and Springfield Faults (faults 42-46 in Fig. 2a and the Appendix), the latter three new since the 1999 report.

Faults in the northeast of the region (Fig. 2b) have been modelled (Russ Van Dissen, pers comm. 2006) in such a way that they allow for slip rate transfer from the Hope Fault to the offshore faults, whereas the absence of the latter in the 1999 model meant that fault sources and the associated slip rates abruptly terminated near the coast. The northeastern section of the Hope Fault is modelled by the Hope-Conway (fault 13) and Hope-Conway-offshore (fault 14) segments, with slip rates of 15 mm/yr and 5 mm/yr respectively. These faults are concurrent along the 81 km length of the Hope-Conway section, with the Hope-Conway-offshore segment continuing a further 40 km offshore. The 15 mm/yr slip rate of fault 13 is transferred to the combined Jordan Thrust-Kekerengu-Chancet Faults (faults 16 and 17), with the northeasterm part of the Kekerengu-Chancet system (fault 15) also modelled to take up the 1 mm/yr slip rate of the Fidget Fault (fault 18), immediately to the west. The Jordan-Kererengu-Chancet Fault consists of two concurrent segments with a combined slip rate of 15 mm/yr, most of this on a blind segment (fault 17) with the top surface at 3 km depth, with only 3.1 mm/yr of the slip rate being carried to the surface by the wider source (fault 16). A map showing these fault geometries is shown in Figure 2b. In general, the balancing of both slip rate along fault systems, and restoration of the plate motion rate across the region are important consideration in the new Canterbury PSH model.

Further south, the faults of the Waitaki and Mackenzie areas have seen major updates as a result of seismic loading studies for hydroelectric power facilities (Berryman *et al.* 2002). The Wharekuri, Rostrievor-Big Gully, Otematapaio and Dryburgh SE Faults used in the 1999 report have been eliminated in the new model, largely through the interpretation of new field data, and the process of amalgamation to form longer sources as a result of our new methodology (Fig. 2 and Appendix). The most obvious example of this process is the new Ostler

Fault source (fault 56), a single source which amalgamates the three Ostler Fault sources defined in the 1999 report. Our methodology produces recurrence intervals that best match the paleoseismically-derived estimates of recurrence interval when a single through-going Ostler Fault source is defined, as opposed to the very short recurrence intervals produced by the segmented model in the 1999 report.

Distributed Earthquake Sources

In addition to defining the locations, magnitudes and frequencies of large (M ~7 - 7.9) to great (M $\geq$ 8) earthquakes on the crustal faults, we also allow for the occurrence of moderate-to-large "distributed" earthquakes (M5 - 7.0) both on and away from the major faults. Our reasons for considering distributed earthquakes in our PSHA are two-fold. First, earthquakes of M < 6.5 often occur on fault sources that have no surface expression, and have therefore escaped mapping by geologists. This is because the rupture widths of these earthquakes are usually less than the width of the seismogenic zone (e.g., Wesnousky, 1986). Second, since many historic M $\geq$ 6.5 earthquakes have not been able to be assigned to specific faults, the possibility exists that some future large earthquakes may also occur on faults not listed in the Appendix.

Our input data and methodology for characterizing the PSH from distributed earthquakes have been significantly updated since the 1999 model. We continue to use the same overall approach, in that the b-value of the Gutenberg-Richter distribution,

$$\log N = a - bM \qquad (7)$$

(in which N = number of events $\geq$ magnitude M, and a and b are empirical constants; Gutenberg & Richter, 1944) is calculated for each of the seismotectonic regions shown in Figure 4, and the a-value is calculated for each grid cell. However, the seismotectonic zones are now based on those used for the national seismic hazard model (Stirling *et al.* 2002). The model now incorporates seismicity data past 1997 (the cutoff year for the 1999 model) and up to 2005, and the a-value has been recalculated according to an adaptive kernel method (Stock & Smith, 2002). The adaptive kernel method allows the smoothing parameters for the a-value to vary according to the spatial distribution of seismicity, rather than simply using one set of parameters as in the 1999 model. Furthermore, the final a-value for each grid cell used in the PSHA is a maximum-likelihood estimate (Stirling *et al.* 2002) based on the various sub-catalogues identified in the New Zealand earthquake catalogue, a sub-catalogue being a space-time subset of the catalogue with a complete record above a specific magnitude threshold. In contrast, the 1999 model used the maximum a-value from any of the identified sub-catalogues as the final a-value, which created unusually high assigned hazard levels in areas where some of the early historical moderate-to-large earthquakes were located (e.g. vicinity of Cheviot and Murchison in Stirling *et al.* 1999).

Attenuation Model

The attenuation relationships used in this study are the same as were used in the 1999 study (now published in McVerry *et al.* 2006). The model provides 5% damped acceleration response spectra (SA(T)) from a data set of New Zealand earthquakes, and takes account of the different tectonic types of earthquakes in New Zealand (restricted to crustal earthquakes for the Canterbury region and surrounds). The attenuation expressions for crustal earthquakes have further subdivisions, through mechanism terms, for different types of fault rupture (strike-slip, normal, oblique/reverse and reverse). The McVerry model is therefore used in this study because it has specific relevance to New Zealand conditions, and makes use of all the available New Zealand strong-motion data that satisfy Quality Assurance selection criteria. It also uses some digital seismograph records converted to accelerograms to increase the number of rock records available. The New Zealand dataset lacks records in the near-source region, at distances of less than 11 km from the earthquake source, and at magnitudes greater than M_w 7.23. Accordingly, some constraints have been applied to the attenuation models for the near-source regions, and for large magnitudes. For PGA, this has been done by supplementing the New Zealand records with 66 overseas records at distances of 10 km or less from the source, and including them directly in the regression analysis for determining the model. In developing the response spectrum model, the approach was to perturb overseas models, constraining some parameters but allowing others to be free in the regression against the New Zealand data. The Abrahamson and Silva (1997) and Youngs *et al.* (1997) models are used as the starting points for the McVerry model for crustal and subduction zone earthquakes, respectively.

The site class terminology used in this report is consistent with that adopted in NZS1170 and Table 3 of McVerry *et al.* (2006). Rock sites are defined as Class A and Class B, Shallow Soil sites as Class C, and Deep or Soft Soil sites as Class D (NZS1170.5:2004; Standards New Zealand, 2004). In this study we calculate all PSH maps and site-specific estimates according to Class C Shallow Soil site conditions.

Computation of Hazard

We use the locations, sizes, and recurrence intervals of earthquakes defined in our source model to estimate the PSH for a gridwork of sites with a grid spacing of 0.1 degrees in latitude and longitude, and calculate site specific estimates for the towns and cities (referred to as centres) of Kaikoura, Christchurch, Timaru and Arthur's Pass. Our measures of PSH are the acceleration levels (stronger horizontal component of PGA, 5% damped response spectral acceleration at 1 second period) and MMI levels with return periods of 475 and 1,000 years. A more comprehensive array of maps are shown in Stirling *et al.* (2007). For a given site, we: (1) calculate the annual frequencies of exceedance for a suite of ground motion levels for every possible earthquake from the magnitude, recurrence interval, and source-to-site distance of earthquakes predicted from the source model; (2) sum the results of (1) across all earthquakes to give the annual frequencies of exceedance for a suite of ground motion levels at the site due to all sources (i.e. the hazard curve), and; (3) find the ground motion levels that correspond to annual frequencies of 1/475 and 1/1,000 years (corresponding to the return periods of 475 and 1,000 years) at the site.

In calculating the ground motions expected with a certain return period, we generally assume a Poisson model of earthquake occurrence, in that we base our estimates of hazard on the average time-independent rate of earthquake occurrence on each fault, and do not calculate time-dependent hazard that would take into account the elapsed time since the last earthquake on the fault. Such calculations are generally limited to faults like the San Andreas of California, for which a large amount of paleoseismic data have been gathered (e.g. Working Group of California Earthquake Probabilities, 1995). In the 1999 report we introduced such time-dependent

calculations to the Alpine Fiordland to Kelly segment (fault 7) of the Alpine Fault (e.g. Yetton *et al.*, 1998), and here update these calculations according to the latest estimates of time-dependent probabilities for the fault (Rhoades & Van Dissen, 2003). Annual probabilities of 0.0075 (lognormal), 0.007 (Weibull), and 0.0053 (Inverse Gaussian) are averaged to give a mean annual probability of 0.0066. In our calculation of ground motions with the McVerry *et al.* attenuation model we adopt the standard practice of modern PSHA and take into account the uncertainty in estimates of ground motion from the attenuation model in the calculation of PSH. The general method is to assume that each estimate of ground motion for a particular earthquake calculated with the attenuation equation at a site is the median of a log-normal distribution, with an associated standard deviation. The standard deviations are usually equal to about 0.5 in natural log units of ground motion. The median and standard deviation are then used to estimate the probability of exceedance for a suite of ground motion levels, with the probabilities of exceedance for each ground motion level multiplied by the earthquake rate to obtain the contribution of the earthquake to the overall exceedance rate of the ground motion at the site. The maps of MMI are calculated according to the methodology of Smith (2003), which uses Monte Carlo methods and MMI attenuation expressions to develop MMI hazard curves. This represents a significant improvement over the simplistic method of using a regression equation to convert from PGA to MMI in the 1999 report. The updated methodology is an extremely important component of the Stirling *et al.* (2007) study, given that the MMI maps produced in the 1999 report were the most frequently used maps in the years following completion of the 1999 report (various ECan staff, pers comm. 1999-2002).

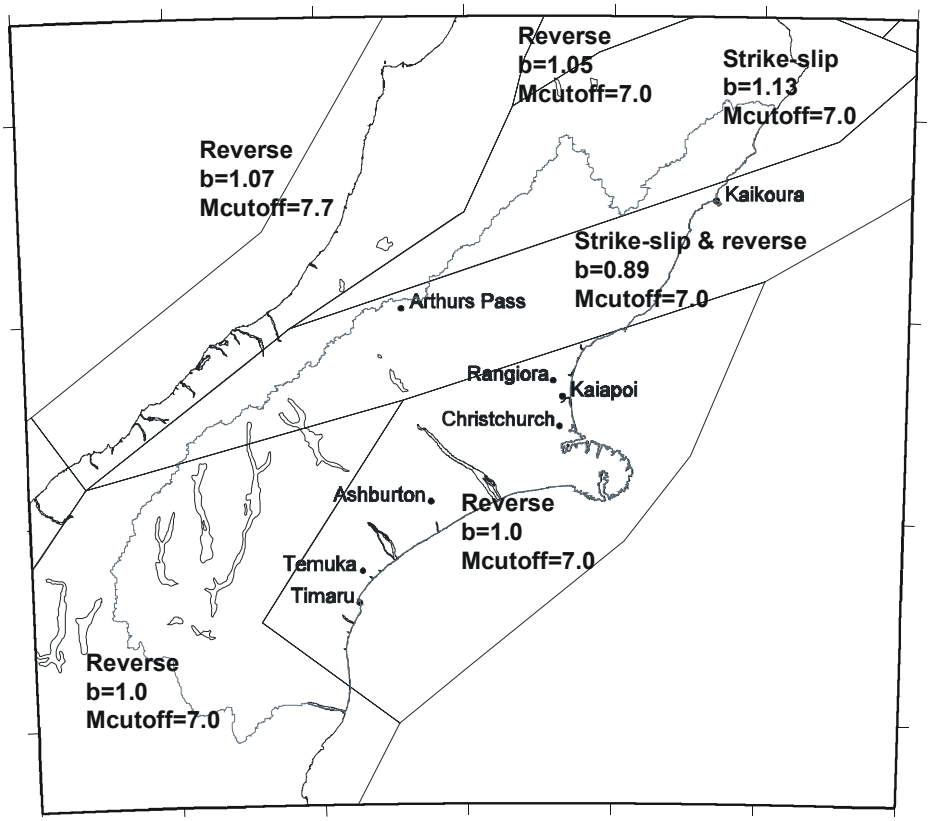

Figure 4. ***Seismotectonic zones used for modelling the distributed seismicity input to the probabilistic seismic hazard analysis (PSHA). The zones are the same as those used in the national seismic hazard model (Stirling et al. 2002) and the updated national model (currently in preparation). The predominant slip-type, the Gutenberg-Richter parameters b (the b-value) and Mcutoff (the maximum magnitude modelled in the distributed seismicity model) are shown on the figure.***

Hazard Estimates

In Figure 5 we show maps of the levels of PGA, 5% damped response spectral acceleration (1 second period) and MMI estimated for the Canterbury region for return periods of 475 and 1,000 years (Figs. 5a-f). In the case of 475 year PGA we also show the equivalent map from the 1999 report for comparison (Fig. 5g). We also show example response spectra for the centres of Kaikoura, Christchurch and Timaru (Fig. 5h).

The maps show very different levels of estimated hazard across the Canterbury region (Fig. 5). In general the highest accelerations and MMIs tend to occur in the north through to southwest of the region. These areas are in the vicinity of Arthur's Pass and Kaikoura, where major active faults are located (Alpine Fault, Kelly Fault, Hope Fault, Jordan Thrust, Kekerengu Fault and associated faults, and the offshore continuations). These are faults that accommodate most of the slip rate of the plate boundary. The highest levels of historical seismicity in the region occur in the central Southern Alps and

northeastern Canterbury (Fig. 3). PGAs of over 0.4g and MMIs of over 8 are estimated for these areas at the 475 year return period. The fault sources tend to have a more significant contribution to the hazard than the distributed sources for long spectral periods and long return periods. Distributed seismicity only really dominates the hazard beyond the northern boundary of the region (Buller area), where faults are generally of low activity (recurrence intervals in the thousands to tens of thousands of years), but large historical earthquakes have occurred and then been followed by a high rate of seismicity to the present day (e.g. Stirling *et al*. 2002).

The overall regional pattern of estimated hazard has not changed greatly from the 1999 report, in that the areas of highest hazard are situated in the north and west of the region where the major plate boundary faults are located (compare Fig. 5a and g). However, there is an overall reduction in hazard over significant parts of the region from the 1999 report. Reductions of 0.1 to 0.2g (or more) are evident in the western Canterbury Plains and eastern Southern Alps. In general the reduced hazard is due to the overall reduction in the number of fault-derived earthquakes in the new fault source model. Fewer fault sources translate to fewer large earthquakes in the PSH calculations. Another significant reduction in hazard on the 475 year PGA map is to the northeast of the Canterbury Plains, and in the neighbouring Buller area to the north. This is mainly due to the maximum-likelihood model-derived a-values in the new distributed seismicity model producing lower hazard than the a-values developed in the 1999 model, and also due to the simplifying of the segmentation model (and consequent reduction of earthquake recurrence rates) for the Porters Pass Fault zone to the northwest of Christchurch (Porters to Grey source, or fault 40). The maps of MMI also show a decrease of up to 1 MMI unit from those of the 1999 report, reflecting the application of the Smith (2003) methodology to the new MMI maps. The only obvious increase in estimated hazard is to the immediate northeast of Kaikoura, where the new offshore sources and slip rate balancing of the faults in that area have increased the earthquake rates and consequent hazard.

We show in Table 1 the values of PGA and spectral acceleration (for a range of spectral periods) and MMI expected at the selected towns or cities of Canterbury, for a range of return periods. Each row represents a response spectrum for a given return period. Example response spectra from Table 1 are also shown in Figure 5h. Clearly, there are considerable differences in hazard for the centres. The highest estimates of PGA, spectral acceleration and MMI are for Kaikoura township. This is not surprising, since Kaikoura is close to the most active faults sources in our PSHA. Both towns are also situated within or near to zones of high distributed seismicity rates. In contrast, the other centres are generally located away to the southeast of the fault sources and areas of high distributed seismicity, so the hazard at these cities and towns is considerably less than for Kaikoura. In general the hazard estimates for the centres have reduced from those of the 1999 report.

The hazard at Christchurch is roughly intermediate for the selected centres. The 475 year PGA estimated for the city is 0.31g, 0.36g less than Arthur's Pass (0.67g), and about 0.05g greater than Timaru (0.26g). Second, our 475 year return period estimate of PGA (0.31g) is slightly less than the equivalent estimate from the 1999 report (0.37g). Several factors contribute to the differences between present and 1999 results. The maximum-likelihood model-derived a-values in the new distributed seismicity model will have produced lower rates of distributed earthquakes in the Cheviot area (site of several moderate-sized early historical earthquakes), and simplifying of the segmentation model for the Porters Pass Fault zone (Porters to Grey source, fault 40) will have reduced the overall estimated recurrence rate of moderate to large earthquakes immediately northwest of the city. Changes to these sources collectively control the small change to the estimated hazard of Christchurch. In all parts of the region reductions or increases in hazard from the 1999 report are reflected to the greatest extent at the long return periods (475 and 1,000 years).

Table 1. Location-specific PGA (Period T = 0.0 sec), and response spectral acceleration (T = 0.075 to 3.0 sec) and MMI (last row) for various return periods (see column 1), and for class C (shallow soil) site conditions. The centres are listed in alphabetical order.

Christchurch
Latitude 43.53S Longitude 172.64E

T(s)	0.00	0.075	0.10	0.15	0.20	0.25	0.30	0.35	0.40	0.50	0.75	1.00	1.50	2.00	3.00
20 yrs	0.07	0.10	0.12	0.14	0.17	0.17	0.17	0.16	0.16	0.13	0.09	0.05	0.04	0.03	0.01
50 yrs	0.11	0.18	0.21	0.26	0.31	0.30	0.29	0.27	0.26	0.22	0.14	0.09	0.07	0.05	0.03
75 yrs	0.14	0.23	0.27	0.32	0.37	0.36	0.34	0.32	0.30	0.25	0.16	0.11	0.08	0.06	0.04
200 yrs	0.22	0.41	0.49	0.55	0.62	0.56	0.52	0.48	0.44	0.37	0.24	0.16	0.12	0.09	0.06
475 yrs	0.31	0.61	0.75	0.82	0.89	0.78	0.71	0.64	0.58	0.48	0.31	0.21	0.15	0.12	0.09
1,000 yrs	0.40	0.83	1.02	1.09	1.17	1.00	0.89	0.79	0.72	0.59	0.38	0.25	0.19	0.14	0.11
2,000 yrs	0.50	1.08	1.34	1.40	1.49	1.25	1.09	0.96	0.86	0.71	0.45	0.31	0.23	0.17	0.14
5,000 yrs	0.64	1.45	1.80	1.85	1.95	1.61	1.37	1.20	1.08	0.88	0.55	0.38	0.29	0.22	0.18
10,000 yrs	0.77	1.76	2.20	2.24	2.34	1.91	1.61	1.40	1.24	1.02	0.63	0.43	0.33	0.25	0.21
20,000 yrs	0.90	2.12	2.65	2.67	2.76	2.23	1.86	1.61	1.43	1.17	0.71	0.48	0.38	0.29	0.24

MMI 50 yrs = 6-7; 150 yrs = 7-8; 475 yrs = 7-8; 1,000 yrs = 8-9

Table 1 continued:

Kaikoura
Latitude 42.41S Longitude 173.69E

T(s)	0.00	0.075	0.10	0.15	0.20	0.25	0.30	0.35	0.40	0.50	0.75	1.00	1.50	2.00	3.00
20 yrs	0.11	0.18	0.21	0.25	0.29	0.28	0.27	0.25	0.24	0.20	0.12	0.08	0.05	0.04	0.02
50 yrs	0.20	0.36	0.44	0.50	0.55	0.51	0.48	0.45	0.42	0.35	0.22	0.14	0.10	0.07	0.04
75 yrs	0.26	0.47	0.58	0.65	0.71	0.65	0.61	0.55	0.52	0.44	0.27	0.18	0.12	0.09	0.06
200 yrs	0.47	0.92	1.17	1.29	1.40	1.21	1.07	0.96	0.87	0.77	0.48	0.34	0.22	0.17	0.11
475 yrs	0.67	1.36	1.79	1.99	2.17	1.81	1.54	1.36	1.22	1.09	0.69	0.50	0.33	0.25	0.16
1,000 yrs	0.84	1.76	2.35	2.64	2.90	2.35	1.96	1.71	1.51	1.35	0.87	0.64	0.44	0.33	0.22
2,000 yrs	1.02	2.19	2.96	3.34	3.71	2.94	2.40	2.07	1.82	1.62	1.06	0.80	0.55	0.41	0.28
5,000 yrs	1.24	2.78	3.81	4.34	4.84	3.74	2.99	2.55	2.21	1.96	1.31	1.00	0.70	0.52	0.38
10,000 yrs	1.42	3.26	4.53	5.18	5.85	4.40	3.46	2.93	2.53	2.23	1.51	1.16	0.82	0.62	0.46
20,000 yrs	1.61	3.79	5.34	6.16	7.07	5.12	3.97	3.34	2.86	2.51	1.72	1.34	0.96	0.72	0.55

MMI 50 yrs = 7-8; 150 yrs = 8-9; 475 yrs = 9-10; 1,000 yrs = 9-10

Timaru
Latitude 44.40S Longitude 171.26E

T(s)	0.00	0.075	0.10	0.15	0.20	0.25	0.30	0.35	0.40	0.50	0.75	1.00	1.50	2.00	3.00
20 yrs	0.05	0.07	0.08	0.09	0.11	0.11	0.11	0.11	0.10	0.08	0.05	0.03	0.02	0.02	0.01
50 yrs	0.09	0.13	0.15	0.19	0.22	0.21	0.21	0.19	0.18	0.15	0.10	0.06	0.04	0.03	0.02
75 yrs	0.11	0.17	0.20	0.24	0.27	0.26	0.25	0.24	0.22	0.19	0.12	0.08	0.05	0.04	0.02
200 yrs	0.18	0.32	0.38	0.43	0.48	0.44	0.41	0.38	0.35	0.30	0.19	0.12	0.09	0.07	0.04
475 yrs	0.26	0.50	0.60	0.66	0.72	0.64	0.58	0.52	0.48	0.40	0.26	0.17	0.12	0.09	0.07
1,000 yrs	0.34	0.69	0.85	0.90	0.96	0.84	0.75	0.67	0.61	0.50	0.32	0.21	0.16	0.12	0.09
2,000 yrs	0.44	0.92	1.14	1.19	1.25	1.06	0.93	0.83	0.75	0.61	0.39	0.26	0.20	0.14	0.12
5,000 yrs	0.57	1.27	1.58	1.61	1.68	1.40	1.20	1.05	0.94	0.77	0.48	0.33	0.25	0.19	0.15
10,000 yrs	0.69	1.57	1.96	1.98	2.05	1.69	1.43	1.25	1.11	0.90	0.56	0.38	0.30	0.22	0.19
20,000 yrs	0.82	1.92	2.39	2.40	2.47	2.00	1.68	1.45	1.29	1.05	0.63	0.43	0.34	0.25	0.22

MMI 50 yrs = 6-7; 150 yrs = 7-8; 475 yrs = 7-8; 1,000 yrs = 7-8

Deaggregation of Hazard

An important application of a PSHA is the development of earthquake scenarios for specific sites of importance and target return periods. A scenario earthquake is usually defined as the most realistic damaging earthquake that is expected to impact a site, and this event may be determined in a variety of ways. We construct and examine de-aggregation graphs for Kaikoura, Christchurch and Timaru . Our plots (Fig. 6) show the contribution to the rate of exceedance of the 475 year return period PGA by sources sorted according to magnitudes and source-to-site distance. The height of the magnitude-distance bins (z-axis) represents the contribution to the exceedance rate of the 475 year PGA by each magnitude-distance category.

The de-aggregation plot for Kaikoura shows fault sources to dominate the hazard. The two peaks on Figure 6a correspond to the large earthquakes at close distances produced by the Hope-Conway, Hundalee and Jordan Thrust sources (faults 13-17, and 31; M_w7.3-7.5 at 11 km or less; Stirling *et al.* 2007). Other fault sources, and the distributed seismicity make minimal contributions to the rate of exceedance of the 475 year PGA by comparison. The most significant change is that distributed seismicity makes a lesser contribution to the hazard than in the 1999 report (the area of the graph at M < 7 and distance < 20 km).

In Christchurch and Timaru the contribution to hazard is from an overall similar mix of sources to those of the 1999 report. The distributed seismicity model makes the largest contribution to the 475 year hazard of the two cities, with fault sources making a significant contribution at the largest magnitudes (Fig. 6b and 6c). In Christchurch (Fig. 6b) the new model gives increased contribution from fault sources and decreased impact from distributed seismicity, although the distributed sources are still more important. Peaks on the graph at the largest magnitude end of the graph are attributed to the Cust and Springbank Fault sources beneath the northeastern Canterbury Plains (M6.8 at 25 - 30 km; Stirling *et al.* 2007), and the Porters to Grey and Ashley Fault sources (M7.2 at 30 - 44 km; Stirling *et al.* 2007), slightly further to the northeast to northwest. In the case of Timaru (Fig. 6c), the relative contributions of fault and distributed sources are similar to the 1999 report, in that most of the 475 year hazard comes from distributed seismicity sources. The main fault source peak on the graph is the Hutt-Peel source (fault 49) at M7.2 and distance about 50 km (Stirling *et al.* 2007). The exact mix of earthquakes making up the de-aggregation plots has therefore changed slightly with our update of the source model. Kaikoura shows almost all the hazard to come from large earthquake sources at close distance, which was a clear conclusion from the 1999 report. Christchurch shows hazard to come from a combination of local earthquakes of moderate magnitude, and large earthquakes at distances of around 50 km. It is also important to note that Alpine Fault earthquakes are also likely to contribute significantly to the hazard for longer spectral periods (T > 0.5 sec) in the centres, so a great Alpine Fault earthquake should still be considered as a realistic scenario earthquake.

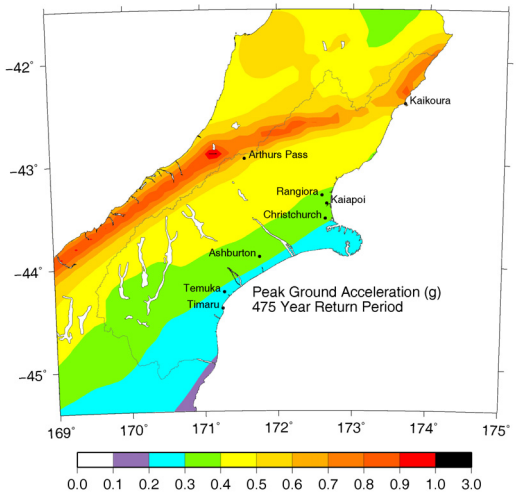

Figure 5a

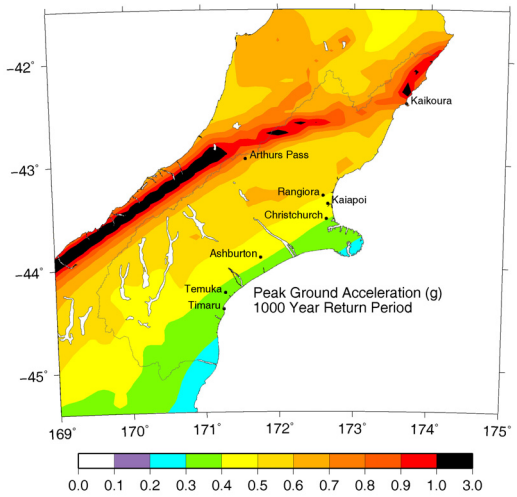

Figure 5b

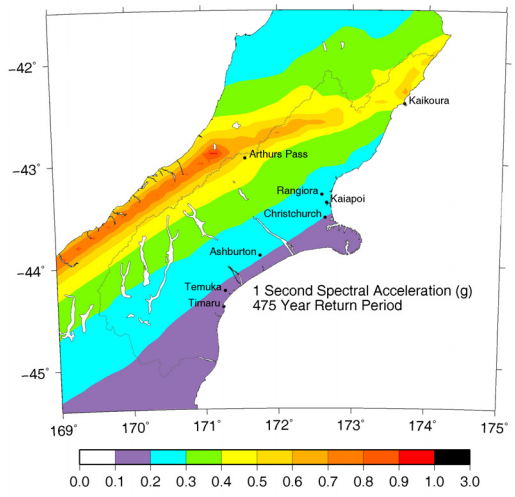

Figure 5c

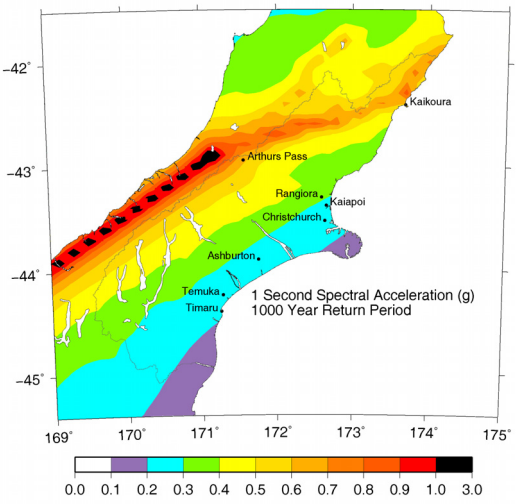

Figure 5d

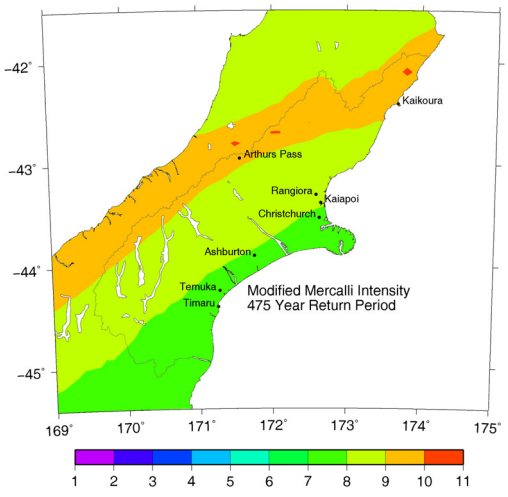

Figure 5e

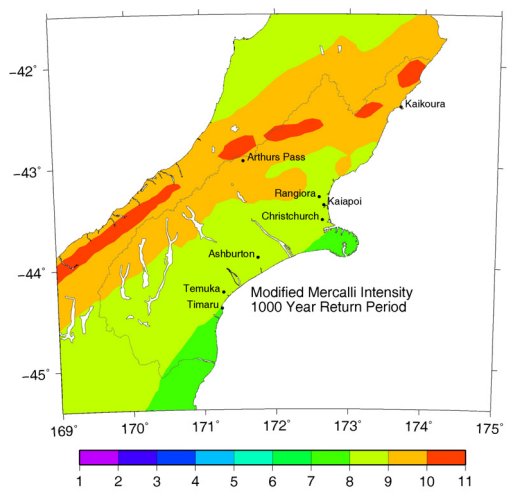

Figure 5f

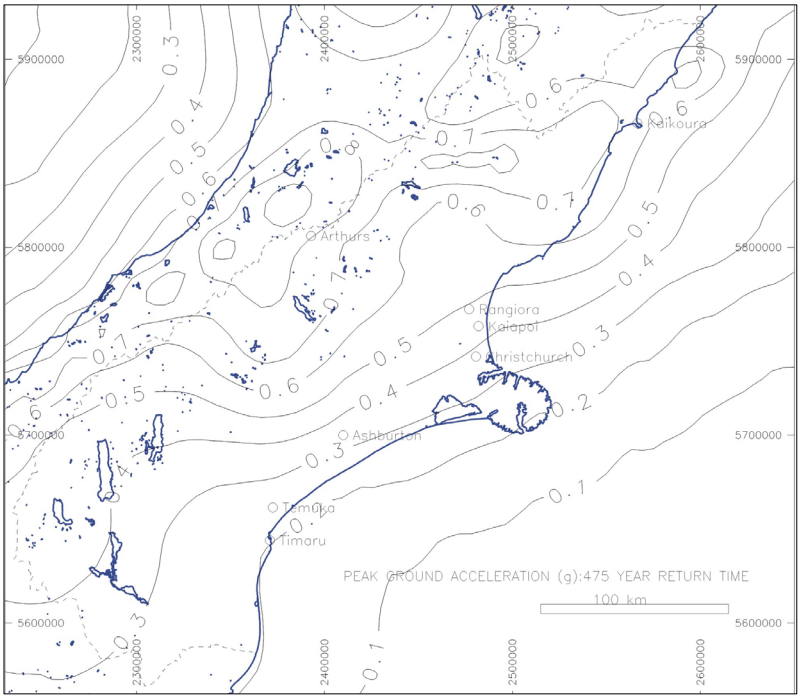

Figure 5g

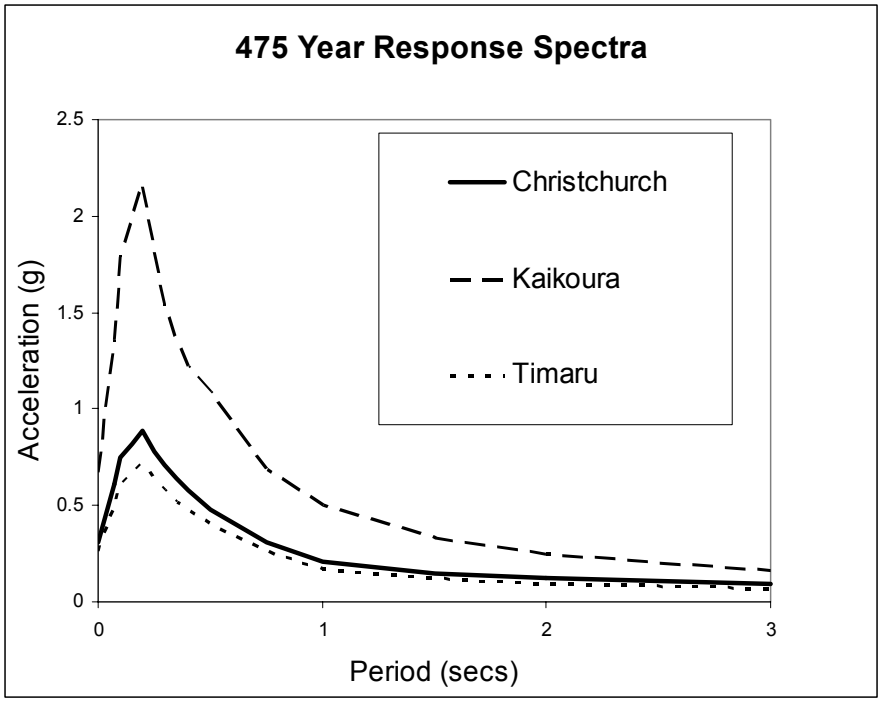

Figure 5h

Figure 5a-h. ***Probabilistic seismic hazard (PSH) maps of the Canterbury region. The maps show the levels of peak ground acceleration (PGA) and spectral acceleration (1 second period) for return periods of 475 and 1000 years on Class C (shallow soil) site conditions of McVerry et al. (2006). The accelerations are in units of g. Modified Mercalli Intensity (MMI) maps are shown for the same return periods. The maps are in order of PGA (a & b), 1 second spectral period (c & d), and MMI (e & f). We also show a 475 year PGA map from the 1999 report for comparison (g), and example response spectra from the NEW PSH model for Kaikoura, Christchurch and Timaru (h; simply a graph of the 475 year return period accelerations from Table 1).***

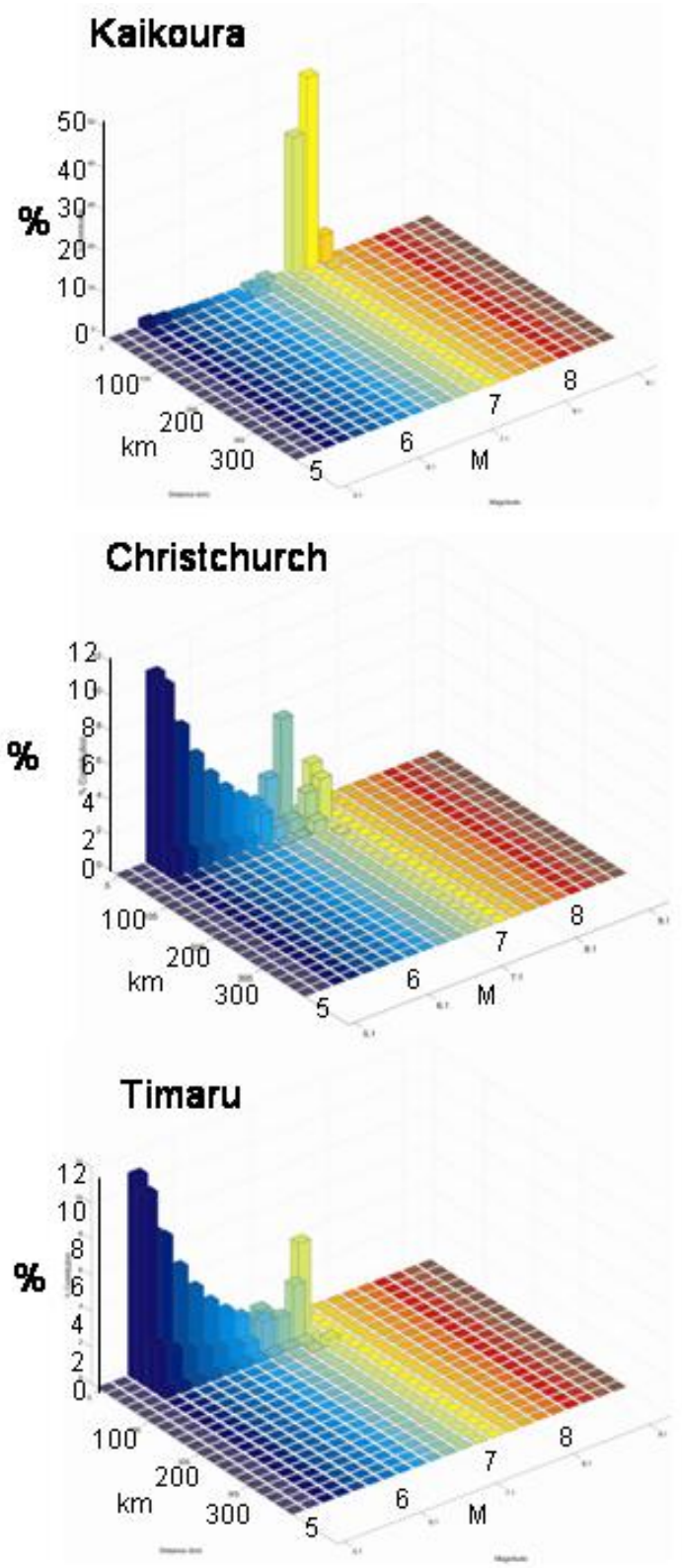

Figure 6 ***De-aggregation graphs showing the magnitude-distance contributions to the annual frequency of exceedance of the 475 year return period PGA at Kaikoura, Christchurch, and Timaru. The distance axis is labelled with "km", magnitude with "M", and percentage contribution to hazard with "%".***

SUMMARY AND CONCLUSIONS

Our update of the Canterbury seismic hazard model has incorporated new onshore and offshore fault data, new seismicity data, new methods for the earthquake source parameterisation of both datasets, and new methods for estimating hazard in terms of MMI. This paper has provided: (1) a PSHA of the Canterbury region, including location–specific PSHAs for Shallow Soil site conditions for selected centres in the region; and (2) de-aggregation information for these centres. While the overall pattern of estimated hazard has not changed since the 1999 report, there has been a slight reduction in estimated hazard over a significant proportion of the western Canterbury Plains and eastern Southern Alps. The new data and parameterisation of the fault source model, new distributed seismicity model, and new methods of estimating MMI are responsible for the differences in hazard from the 1999 study. Given the relatively minor changes to the PSH estimates from those of the 1999 report, future significant regional changes to the Canterbury PSH model are likely to come from factors other than the update of the source model, such as incorporation of detailed site condition information, or a completely different modelling approach.

ACKNOWLEDGEMENTS

Helen Grant is thanked for permission to publish the results of Stirling *et al.* (2007). Misko Cubrinovski (University of Canterbury) is thanked for his review of this paper. We are indebted to the following scientists for contributing their expertise, time and efforts to an intensive review of the recurrence parameters for the Canterbury region faults; Kelvin Berryman, Russ Van Dissen (who's fault model was used directly in Fig. 2b), Robert Langridge, Pilar Villamor, Andy Nicol, Kate Wilson and Roberto Basili.

REFERENCES

Abrahamson, N.A., and Silva, W.J. (1997). Empirical response spectral attenuation relationships for shallow crustal earthquakes. *Seismological Research Letters* **68**, 94-127.

Aki, K., and Richards, P.G. (1980). *Quantitative Seismology: Theory and Methods*, W.H. Freeman, San Francisco, California.

Berryman, K.R., Beanland, S., Cooper, A.F., Cutten, H.N., Norris, R.J., Wood, P.R. (1992). The Alpine Fault, New Zealand: Variation in Quaternary structural style and geomorphic expression. *Annales Tectonicae Suppliment to Volume* **6**: 126-163.

Berryman, K., Webb, T., Hill, N., Stirling, M., Rhoades, D., Beavan, J., Darby, D. (2002). Seismic loads on dams, Waitaki system. Earthquake Source Characterisation. Main report. GNS client report 2001/129.

Berryman, K.R. and Villamor, P.V. (2004). Surface rupture of the Poulter Fault in the 1929 March 9 Arthurs Pass earthquake, and redefinition of the Kakapo Fault, *New Zealand Journal of Geology and Geophysics* **47**: 341-351.

Cornell, C.A. (1968). Engineering seismic risk analysis. *Bulletin of the Seismological Society of America* **58**: 583-1606.

Cowan, H.A., (1991). the North Canterbury earthquake of 1 September, 1888. *Journal of the Royal Society of New Zealand* **21***:*1-12.

DeMets, C., Gordon, R.G., Argus, D.F. and Stein, S. (1990). Current plate motions. *Geophysical Journal International* **101**: 425-478.

Grapes, R., Little, T., and Downes, G. (1998). Rupturing of the Awatere Fault during the 1848 October 16 Marlborough earthquake, New Zealand: historical and present day evidence*. New Zealand Journal of Geology and Geophysics* **41**:387-399.

Gutenberg, B. and Richter, C.F. (1944). Frequency of earthquakes in California. *Bulletin of the Seismological Society of America* **34**: 185-188.

Hanks, T.C. and Bakun, W.H. (2002). A bilinear source-scaling model for M-logA observations of continental earthquakes. *Bulletin of the Seismological Society of America* **92**: 1841-1846.

Hanks, T.C. and Kanamori, H. (1979). A moment magnitude scale. *Journal of Geophysical Research* **84**: 2348-2350.

Howard M. (2001). Holocene surface-rupturing earthquakes along the Porters Pass Fault. Unpublished MSc thesis, University of Canterbury, Christchurch, New Zealand.

Howard, M., Nicol, A., Campbell, J. Pettinga, J.R. (2005). Holocene paleoearthquakes on the strike-slip Porters Pass Fault, Canterbury, New Zealand. *New Zealand Journal of Geology and Geophysics* **48**: 59-74.

Langridge, R. M., Campbell, J., Hill, N. L., Pere, V., Pope, J., Pettinga, J., Estrada, B., Berryman, K. R. (2003). Paleoseismology and slip rate of the Conway segment of the Hope Fault at Greenburn Stream, South Island, New Zealand. *Annals of Geophysics* **46** *(5):* 1119-1139.

McVerry, G.H., Zhao, J.X., Abrahamson, N.A., Somerville, P.G. (2006). New Zealand acceleration response spectrum attenuation relations for crustal and subduction zone earthquakes. *Bulletin of the New Zealand Society of Earthquake Engineering* **38**(1*),* 1-58.

Norris, R. J. and Cooper, A. F. (2001). Late Quaternary slip rates and slip partitioning on the Alpine Fault, New Zealand. *Journal of Structural Geology* **23**: 507-520.

Pettinga, J.R., Chamberlain, C.G., Yetton, M.D., Van Dissen, R.J. and Downes, G. (1998). *Earthquake Hazard and Risk Assessment Study (Stage 1 – Part A); Earthquake Source Identification and Characterisation*. Canterbury Regional Council Publication U98/10.

Pettinga, J.R., Yetton, M.D., Van Dissen, R.J. and Downes, G.D. (2001). Earthquake source identification and characterisation for the Canterbury region, South Island, New Zealand. *Bulletin of the New Zealand Society of Earthquake Engineering* **34**(4), 282-317.

Rhoades, D. A. and Van Dissen, R. J. (2003). Estimates of the time-varying hazard of rupture of the Alpine Fault, New Zealand, allowing for uncertainties. *New Zealand Journal of Geology and Geophysics* **46** (4): 479-488.

Smith, W.D., (2003). Earthquake hazard and risk assessment in New Zealand by Monte Carlo methods. *Seismological Research Letters,* **74**, 298-304.

Standards New Zealand, (2004). Structural Design Actions Part 5 Earthquake Actions – *New Zealand. Standard NZS1170.5*:2004.

Stirling, M.W., Yetton, M., Pettinga, J., Berryman, K. and Downes, G. (1999). Probabilistic seismic hazard assessment and earthquake scenarios for the Canterbury Region, and historic earthquakes in Christchurch. GNS client report 1999/53.

Stirling, M.W., Pettinga, J., Berryman, K.R. and Yetton, M. (2001). Probabilistic seismic hazard assessment of the Canterbury region, New Zealand. *Bulletin of the New Zealand Society of Earthquake Engineering* **34**, 318-334

Stirling, M.W., McVerry, G.H., Berryman, K.R. (2002). A new seismic hazard model for New Zealand . *Bulletin of the Seismological Society of America.* **92**, 1878-1903.

Stirling, M.W. and Barnes, P.M. (2003). Seismic hazard model for New Zealand. *Natural Hazards Update 4:* 1.

Stirling, M.W., Gerstenberger, M., Litchfield, N.J., McVerry, G.H., Smith, W.D., Pettinga, J., and Barnes, P. (2007). Updated probabilistic seismic hazard assessment for the Canterbury region. *GNS Science Consultancy Report 2007/232*.

Stock, C. and Smith, E.G.C. (2002). Comparison of seismicity models generated by different kernel estimations. *Bulletin of the Seismological Society of America* **92**, 913-922

Sutherland, R., Norris, R.J. (1995). Late Quaternary displacement rate, paleoseismicity, and geomorphic evolution of the Alpine Fault: evidence from Hokuri Creek, South Westland, New Zealand. *New Zealand Journal of Geology and Geophysics* **38***:* 419-430.

Sutherland, R., Berryman, K. R., Norris, R. J. (2006a). Displacement rate on the Alpine Fault determined from offset glacial landforms between Milford Sound and the Cascade Valley: implications for the kinematics and seismic hazard of southern New Zealand. *Geological Society Of America Bulletin* **118***(3/4):* 464-474.

Sutherland, R., Eberhart-Philips, D., Harris, R.A., Stern, T., Beavan, J., Ellis, S., Henrys, S., Cox, S., Norris, R.J., Berryman, K.R., Towend, J., Bannister, S., Pettinga, J., Leitner, B., Wallace, L., Little, T.A., Cooper, A.F., Yetton, M., Stirling, M.W. (2006b). Do great earthquakes occur on the Alpine fault in central South Island, New Zealand? *Geophysical Monograph, SIGHT. American Geophysical Union*.

Villamor, P., Berryman, K., Webb, T., Stirling, M., McGinty, P., Downes, G., Harris, J., Litchfield, N., (2001). Waikato seismic loads - Task 2.1. Revision of seismic source characterisation. GNS client report 2001/59.

Wesnousky, S.G. (1986). Earthquakes, Quaternary faults and seismic hazard in California. *Journal of Geophysical Research* **91**: 12587-12631.

Working Group of California Earthquake Probabilities, (1995). Seismic hazards in southern California, probable earthquakes 1994-2004. *Bulletin of the Seismological Society of America* **85**, 379-439.

Yetton, M.D., Wells, A., and Traylen, N.J., (1998)*: The probability and consequences of the next Alpine Fault earthquake.* EQC Research Report 95/193.

Youngs, R.R., Chiou, S.J., Silva, W.J. and Humphrey, J.R. (1997). Strong ground motion attenuation relationships for subduction zone earthquakes, Seismological Research Letters, **68**(1), 58-73.

Appendix — Fault Sources

Fault sources used as input to the PSHA. Type is slip type (ss = strike-slip, nn = normal, rv = reverse, and variants of these indicate oblique-slip), Length is predicted rupture length (km), and ID is the fault source number that corresponds to the fault maps in Figure 2. The full list of fault parameters used in the PSHA, and references used to update the fault sources of the 1999 report can be seen in Stirling *et al.* (2007),

Fault Source	Type	Length	ID
Wairau	ss	103	1
Wairau (Offshore)	ss	93	2
Awatere (SW)	ss	93	3
Awatere (NE)	ss	115	4
Barefell Pass	ss	26	5
Fowlers	ss	53	6
Alpine (Fiord- Kelly)	ss	413	7
Alpine (Kelly-Tophouse)	ss	194	8
Clarence (SW)	ss	75	9
Clarence (NE)	ss	123	10
Clarence (Central)	ss	54	11
Hope (1888 rupture)	ss	44	12
Hope (Conway)	ss	81	13
Hope (Conway Offshore)	ss	121	14
Kekerengu-Chancet	ss	64	15
Jordan-Keke-Chancet	rs	87	16
Jordan-BKeke-Chancet	rs	87	17
Fidget	ss	34	18
Kelly	ss	58	19
Hope (Taramakau)	ss	30	20
Hope (Central-west)	ss	36	21
Kakapo	ss	47	22
Browning Pass	ss	29	23
Poulter	ss	48	24
Paparoa Range front	rv	77	25
Inangahua	rv	38	26
Maimai	rv	39	27
Brunner Anticline	rv	59	28
White Creek	rv	120	29
Lyell	rv	39	30
Hundalee	rv	53	31
Kaiwara North	rv	27	32
Kaiwara South	rv	44	33
Omihi	rv	17	34
Lowry	rv	45	35
Waitohi	rv	37	36
Esk	rs	40	37
Torlesse	rv	51	38
Cheesman	rv	22	39
Porters to Grey	sr	81	40
Lees Valley	rs	26	41
Ashley	rv	52	42
Springbank	rv	26	43
Cust	rv	27	44
Hororata	rv	40	45
Springfield	rv	43	46
Lk Heron-Forest Crk	rv	50	47
Quartz Creek	rs	12	48
Hutt-Peel	rv	64	49
Fox Peak	rv	50	50
Waimea South	rs	40	51
Waimea North	rs	69	52
Pisa	rv	47	53
Nevis	rv	69	54
Wairarapa-Nicholson	sr	140	55
Ostler	rv	68	56
Ahuriri River	rv	44	57
Irishman Creek	rv	40	58
Lindis Peak	rs	38	59
Grandview	rv	32	60
Cardrona South	rv	28	61
Cardrona North	rv	34	62
Blue Lake	rv	41	63
Dunstan	rv	57	64
Raggedy	rv	37	65
Gimmerburn	rv	42	66
Ranfurly	rv	15	67
Waipiata	rv	65	68
LongValley	rv	21	69
Hyde	rv	46	70
Billys Ridge	rv	34	71
Taieri Ridge	rv	35	72
Hanmer	nn	18	73
Ohariu South	ss	55	74
Wellington WHV	ss	75	75
Spylaw	rv	50	76
Blue Mountain	rv	51	77
Old Man	rv	52	78
Dry River-Huangarua	rv	47	79
Otaraia	rv	35	80
Whitemans	rv	28	81
Akatarawa-Otaki Forks	sr	58	82
Moonshine	sr	36	83
Moonlight North	rs	88	84
Moonlight South	rs	100	85
Albury	rv	20	86
Brothers	rv	35	87
Dalgety	rv	25	88
Dryburgh	rv	30	89
Hunter Range Front	rv	50	90
Stonewall	rv	20	91
Kirkliston	rv	35	92
Opawa	rv	30	93

Otematata	rv	17	94
Fern Gully	sr	53	95
Waitangi	rv	36	96
Pegasus 1	rv	32.9	97
North Canterbury1	rv	30.1	98
North Canterbury 2	rv	19.1	99
North Canterbury 4	rv	11.75	100
North Canterbury 11	rv	27.3	101
North Canterbury 8	rv	38.6	102
North Canterbury 10	rv	21.7	103
North Canterbury 13	rv	26.5	104
North Mernoo B0	nn	46.3	105
North Mernoo B1	nn	20.6	106
North Mernoo B2	nn	50.1	107
North Mernoo 4647	nn	40.6	108
North Mernoo E1	nn	41	109
North Mernoo E2	nn	35	110
North Mernoo F1	nn	30	111
North Mernoo F2	nn	34	112
North Mernoo 1819	nn	39.3	113
North Mernoo K1	nn	64	114
North Mernoo K2	nn	30	115
North Mernoo M	nn	48.97	116
Marlborough Slope 09	rv	15.1	117
Marlborough Slope 04	rv	44.9	118
Marlborough Slope 08	rv	20.5	119
Marlborough Slope 02	rv	14.2	120
Marlborough Slope 01	rv	20.1	121
Marlborough Slope 05	rv	34.5	122
UpperSlope	rv	41.8	123
Marlborough Slope 06	rs	15	124
Te Rapa (segment 1-2)	rs	47	125
Wharanui-Campbell	rs	47	126
Kekerengu-Campbell	rs	42	127
Needles	sn	55	128
Boo Boo	sn	71	129
Long Valley	rv	21	130
Kekerengu Bank	rv	88	131
Pukerua-Shepherds	ss	62	132
Waitohi	rv	37	133